Published in final edited form as:

Nature. 2020 August ; 584(7820): 221–226. doi:10.1038/s41586-020-2565-5.

Coupling Dinitrogen and Hydrocarbons through Aryl Migration

Sean F. McWilliams[1,4], **Daniël L. J. Broere**[1,2,4], **Connor J. V. Halliday**[3], **Samuel M. Bhutto**[1], **Brandon Q. Mercado**[1], **Patrick L. Holland**[1,*]

[1]Department of Chemistry, Yale University, New Haven, Connecticut 06520, United States [2]Current address: Debye Institute for Nanomaterials Science, Utrecht University, 3584 CG Utrecht, The Netherlands [3]EaStCHEM School of Chemistry, University of Edinburgh, The King's Buildings, Edinburgh, EH9 3FJ, United Kingdom [4]These authors contributed equally: Sean F. McWilliams, Daniël L. J. Broere.

Abstract

A persistent challenge in chemistry is to activate abundant, yet inert molecules such as hydrocarbons and atmospheric N_2. In particular, forming C–N bonds from N_2 typically requires a reactive organic precursor[1], which limits the ability to design catalytic cycles. Here, we report an diketiminate-supported iron system that is able to sequentially activate benzene and N_2 to form aniline derivatives. The key to this new coupling reaction is the partial silylation of a reduced iron-N_2 complex, which is followed by migratory insertion of a benzene-derived phenyl group to the nitrogen. Further reduction releases the nitrogen products, and the resulting iron species can re-enter the cyclic pathway. Using a mixture of sodium powder, crown ether, and trimethylsilyl bromide, an easily prepared diketiminate iron bromide complex[2] can mediate the one-pot conversion of several petroleum-derived compounds into the corresponding silylated aniline derivatives using N_2 as the nitrogen source. Numerous compounds along the cyclic pathway have been isolated and crystallographically characterized; their reactivity outlines the mechanism including the hydrocarbon activation step and the N_2 functionalization step. This strategy incorporates nitrogen atoms from N_2 directly into abundant hydrocarbons.

Reduction or "fixation" of N_2 is accomplished by a few catalytic systems[3–8] which fully reduce it to ammonia (NH_3)[9]. It is difficult to adapt these processes to form C–N bonds from

*To whom correspondence should be addressed. patrick.holland@yale.edu.

Author Contributions. S.F.M., D.L.J.B., and P.L.H. conceived of the ideas and designed the experiments. S.F.M., D.L.J.B., C.J.V.H., and S.M.B. performed the experiments. B.Q.M. performed crystallographic measurements and interpretation. S.F.M., D.L.J.B., and P.L.H. wrote the manuscript.

Methods are in the Supplementary Information.

Competing Interests. The authors declare no competing interests.

Supplementary Information is available for this paper: Materials, Methods, Spectroscopic Data, and Additional References (PDF); Crystallographic Information Files (CIF).

Data Availability Statement. Materials and methods, experimental procedures, useful information, spectra and MS data are available in the Supplementary Information. Raw data are available from the corresponding author on reasonable request. The crystallographic datasets generated during the current study are publicly available from the CCDC repository, with accession codes 1937999, 1978000, 1938001, 1938002, 1939265, 1939266, and 1966313.

N_2, even though a number of compelling functionalizations of N_2 are thermodynamically feasible[10]. Efforts to form C–N bonds from N_2 generally require reduction of N_2 to make it nucleophilic enough to react with carbon electrophiles[11,12]. Notable examples include synthetic cycles for C–N bond formation from Cummins, Sita, Mori, and Schneider[13–17]. A frequent difficulty is the direct reaction of the reducing agents with the carbon electrophiles.

There would be a substantial advantage if N_2 could be induced to form a C–N bond with a simple hydrocarbon, without prior functionalization of the hydrocarbon to convert it into an electrophile. Such a strategy would require C–H activation of the hydrocarbon, leveraging the decades of work on oxidative addition of C–H bonds by low-valent transition metal complexes[18]. C–H functionalization to form cross-coupling products is well-known[19], but there are no previous examples of cross-coupling of C–H bonds with the relatively unreactive N_2 molecule.

Here, we report an iron complex that couples N_2 and unactivated arenes at low temperature, taking advantage of silyl activation of the N_2 to produce silylated anilines in a one-pot procedure. The overall strategy (Fig. 1) begins with C–H bond activation of benzene to form a phenyl fragment, which could migrate to N_2 upon silylation to form the key C–N bond. To explore the feasibility of this pathway, we converted the iron(II) bromide complex $[LFe(\mu\text{-}Br)]_2$ (**1**) into the iron(I) benzene complex $LFe(\eta^6\text{-}C_6H_6)$ (**2**)[20]. Fig. 2 shows the structure of **2** and illustrates the β-diketiminate ligand L, which controls the coordination environment of iron[21]. Reduction of **2** with KC_8 in the presence of 18-crown-6 (18c6) at room temperature led to the isolable, purple iron(0) complex $LFe(\eta^4\text{-}C_6H_6)K(18c6)$ (**3-K**)[2]. When **2** was reduced instead with Na and 15-crown-5 (15c5) in benzene, the product was the red iron(II) complex LFe(H)(Ph)Na(15c5) (**4-Na**), in which a C–H bond of benzene is broken to give an iron(II) complex with phenyl and hydride groups on the iron (Fig. S50). Thus, **3-K** and **4-Na** have isomeric anions (top of Fig. 2A). Mössbauer spectra of solid **3-K** and **4-Na** (Fig. S23–S25) support the difference, and density functional theory (DFT) studies indicate that the molecules have high-spin electronic configurations ($S = 1$ for **3-K** and $S = 2$ for **4-Na**). This is a rare case of room-temperature C–H activation using a high-spin iron complex[22,23]. Reduction of **2** with Na and 15-crown-5 in toluene similarly gave LFe(H)(Tol)Na(15c5), from activation of the aryl C–H bonds of the solvent. The X-ray crystal structure refined best to a 61:39 mixture of meta and para isomers (Fig. S54).

The solution ^{1}H NMR (nuclear magnetic resonance) spectra of **3-K** and **4-Na** in C_6D_6 showed a few peaks that disappeared over several hours, suggesting that these benzene or phenyl groups exchange with C_6D_6. Additionally, a minor component was observed in the ^{1}H NMR spectrum of the C_6D_6 solutions of **3-K** that resembled those of **4-Na**, and vice versa. These observations suggested that arene-bound iron(0) complex **3** and C-H activated iron(II) complex **4** are in equilibrium with one another, and the iron(0) arene isomer (**3**) predominates with $K(18c6)^+$, while the oxidatively added iron(II) phenyl hydride isomer (**4**) predominates with $Na(15c5)^+$ (see Tables S7–S8). This hypothesis was strongly supported through solution studies in THF (tetrahydrofuran), a solvent that can disrupt the interactions with the alkali metal. Dissolving either purified **3-K** or purified **4-Na** in THF gave mixtures with characteristic peaks of both isomers **3** and **4** in ^{1}H NMR and Mössbauer spectra (Fig.

S9, S26). The ability of each isomer to produce the other one demonstrates that there is reversible oxidative addition of the aryl C–H bond of **3** to form **4**.

Purple THF solutions of LFe(H)(Ph)Na(15c5) (**4-Na**) turned green upon standing at room temperature for several hours, and ^{1}H NMR spectra showed formation of the iron(I) phenyl complex [LFePh][Na(15c5)] (**6-Na**) (Fig. 2B). Though the formation of **6-Na** from **4-Na** corresponds to formal loss of H•, the spectroscopic yield of **6-Na** from **4-Na** in THF was only 18% (Fig. S17), and the best yield of **6-Na** (44%) came from addition of excess 15c5 and Na to **2** in diethyl ether (Fig. S18). These results suggested that the reaction could have a different pathway. In a mechanistically revealing experiment, **4-Na** transferred the hydride to BPh_3 (triphenylborane) to give **5** and [Na(15c5)][$HBPh_3$] (Fig. S19–S20) in a higher yield of 75%. Therefore, it is possible that in the presence of excess reducing agent, **4-Na** can similarly lose hydride to give **5**, which is subsequently reduced by **3** or by Na to give the observed **6-Na**.

Next, we explored N_2 binding. Cooling a solution of **6-Na** in THF under an atmosphere of N_2 led to changes in the electronic absorption (UV-vis) spectrum (Fig. 3A) and Mössbauer spectrum (Fig. 3B) that did not occur in control experiments under argon. Van't Hoff analysis of the UV-vis data for **6-Na** gave $\Delta H = -17 \pm 2$ kJ mol^{-1} and $\Delta S = -55 \pm 10$ J K^{-1} mol^{-1} (Fig. S40), which are consistent with the binding of N_2. In order to gain crystallographic verification of N_2 binding, we cooled a concentrated sample of the potassium analogue **6-K** at −78 °C for 3 h, which led to crystals of the N_2 complex **7-K**. The X-ray crystal structure of **7-K** (within Fig. 4 below) demonstrates end-on binding of the N_2 unit and a pseudotetrahedral geometry at the iron(I) site, and the spectroscopic similarity to the Na system (Figs. S36–S39) indicates that **7-Na** has a similar structure.

Next, we silylated the N_2 ligand that had been activated through Fe coordination. Treating a cold solution of **7-K** with 2 equivalents of Me_3SiX (X = Br, I) formed the hydrazido complex LFe(N(Ph)N($SiMe_3$)$_2$) (**8**). To our knowledge, the transformation of **7** to **8** is the first crystallographically-verified example of the migration of a hydrocarbyl group from a metal to the α position of N_2[25–26]. This is the key C–N bond forming step during the formation of silylated anilines (Fig. 1), which differs from the previously utilized attacks on bound N_2 by carbon electrophiles.

Though we did not detect any intermediates during the conversion of **7** to **8**, the treatment of a cold solution of **7-K** with 0.5 molar equivalents of the bulkier triisopropylsilyl triflate (TIPSOTf; OTf = SO_3CF_3) gave the formally iron(II) diazenido complex **9**, in which the N_2 is singly silylated while the phenyl group remains bound to the iron (Figure S55). The conversion of **7** to **9** is accompanied by a similar yield of the iron(II) complex **5**, which results from half of **7** acting as a reducing agent. Considering this stoichiometry, the formation of **9** occurs in 67% yield. The isolation of **9**, in which the phenyl has not migrated, suggests that the initial silylation of the β position of the coordinated N_2 in **7** takes place before the migration of the aryl group. It is likely that the second silylation induces the aryl migration, because Peters recently reported the migration of H from an iron center to the α position of a doubly silylated N_2 group to form an iron disilylhydrazido complex[27]. Accordingly, addition of excess trimethylsilyl triflate (Me_3SiOTf) and excess Na to **9** gave a

14% yield of $PhN(SiMe_3)_2$, showing that addition of a second silyl group can initiate C–N bond formation. This could be because the second silylation leads to a formally iron(IV) complex with a Fe=N double bond, a migration that is reminiscent of alkyl migration to N in an imidoiron(IV) complex[28].

The conversion of **8** to the silylated aniline and amine occurred upon the addition of 1 equivalent of KC_8 and 2 equivalents of Me_3SiX (X = Br, I) to solutions of **8**: this treatment led to mixtures containing $PhN(SiMe_3)_2$, $PhN(SiMe_3)N(SiMe_3)_2$ and $N(SiMe_3)_3$ within 30 min, either at room temperature or at −100 °C. In contrast, **8** did not react with 2 equivalents of Me_3SiBr alone within 3 days at room temperature. This result suggests that reduction precedes the electrophilic attack of silyl groups on **8**, and alternatively this final step could involve the formation of $Me_3Si^{\bullet}$ radicals[28,30]. Others have also studied the reductive silylation of disilylhydrazido complexes[30,31].

After release of the silylated nitrogen products from **8**, the large excess of bromide is expected to give iron(II) bromide species that are poised to be reduced with further arene binding. This suggests the feasibility of a cyclic process (Fig. 4) in a single pot, which forms silylated anilines from arenes and N_2. However, the C–H activation and hydride loss to reform complex **6** requires room temperature treatment with Na, and at this temperature Na degrades Me_3SiBr. Further, N_2 binds to **6** at low temperatures. Thus, we treated **8** with Na (25 equivalents), benzene (20 equivalents), Me_3SiBr (6 equivalents), and 15c5 (5 equivalents) at −100 °C in diethyl ether, then warmed to room temperature for 1 h, then cooled again and treated with additional Me_3SiBr (6 equivalents). This led to a 92% yield of $PhN(SiMe_3)_2$ and a 135% yield of $N(SiMe_3)_3$ (yields *vs.* Fe). In order to verify that the overall process is indeed cyclic, **8** was treated with the same conditions with added toluene in place of benzene. Analysis of the organic reaction products after two cycles of Me_3SiBr addition showed a 163% yield of $N(SiMe_3)_3$, a 62% yield of $PhN(SiMe_3)_2$, and a 16% yield of $(tolyl)N(SiMe_3)_2$ (both meta and para isomers). The ability of the phenylhydrazido complex to give products from toluene amination demonstrates that the iron containing products of the hydrazido reduction can activate toluene and continue to another reaction cycle, though the yields are low.

To test the overall cycle, we reacted the easily-prepared iron(II) complex **1** with 30 molar equivalents (equivalents relative to [Fe]) of Na, 20 equivalents of C_6H_6, and 5 equivalents of 15c5 at ambient temperature in diethyl ether, followed by addition of 6 equivalents of trimethylsilyl bromide (Me_3SiBr) at −108 °C, afforded $PhN(SiMe_3)_2$ in a yield of 24% per iron atom as determined by gas chromatography (GC). The yield of the reaction could be increased by adding the Me_3SiBr in several portions with temperature cycling. First, a mixture of **1**, 35 equivalents of Na, 20 equivalents of benzene, and 5 equivalents of 15c5 in diethyl ether was stirred vigorously for 1.5 hours at room temperature until it became green, corresponding to the color of **6**. Cooling the mixture to −108 °C under 1 atm N_2 resulted in a color change to dark red, corresponding to **7**. Then, addition of 2 equivalents of Me_3SiBr (per iron) to this cold solution and warming to room temperature for 1 hour resulted in another green reaction mixture, suggesting that **6** was regenerated. Cooling again caused the same color change to red (**7**), and more Me_3SiBr was then added in a second cycle. Repeating 10 cooling/silylation/warming cycles with 2 equivalents of Me_3SiBr per cycle

gave a cumulative yield of 85 ± 14% of $PhN(SiMe_3)_2$ (*vs.* Fe; average and standard deviation of 6 trials; Table S1). The ability to produce more product with repeated Me_3SiBr additions suggests a cyclic process, albeit one where a significant amount of the active species decomposes in each cycle. Though aniline formation was attenuated with repeated cycles, the yield of $N(SiMe_3)_3$ continued to increase with the number of additions of Me_3SiBr, reaching 380 ± 41% (*vs.* Fe) (Fig. S1–S2). Under the same conditions but in the absence of benzene, no $PhN(SiMe_3)_2$ was produced yet a similar catalytic yield of $N(SiMe_3)_3$ was observed. Neither product was detected in the absence of **1**. These results suggest that the iron decomposition products lose the ability to aminate benzene, but remain competent for the silylation of N_2 to $N(SiMe_3)_3$, a more common reaction that has been reported with other homogeneous catalysts and decomposition products[32–40].

Isotope labeling experiments were used to verify that the aniline product arises from benzene and N_2. When performing the reaction under an atmosphere of $^{15}N_2$, GC-MS indicated the formation of $Ph^{15}N(SiMe_3)_2$ and $^{15}N(SiMe_3)_3$ (Fig. 5A), demonstrating that N_2 is the source of the N atoms. Performing the reaction with C_6D_6 as the arene substrate gave $(C_6D_5)N(SiMe_3)_2$, showing that benzene is the source of the phenyl group. The reaction with an equimolar mixture of C_6H_6 and C_6D_6 gave a 1:1 mixture of $(C_6H_5)N(SiMe_3)_2$ and $(C_6D_5)N(SiMe_3)_2$ (Fig. 5B), but partially deuterated 1,3,5-d_3-benzene gave $(C_6H_2D_3)N(SiMe_3)_2$ and $(C_6H_3D_2)N(SiMe_3)_2$ in a ratio of 2.01 ± 0.05 indicating a normal primary kinetic isotope effect for the C–H cleavage step. The difference between the intramolecular vs. intermolecular isotope effects[41] indicates that arene binding/exchange is not much more rapid than the irreversible step after C–H cleavage, which is qualitatively consistent with the timescales of the experiments described above with the **3**/**4** equilibrium (which is established over 1–2 hours in diethyl ether) and the formation of **6** (which takes a few hours).

Other arene substrates were also tested using 5 cycles of Me_3SiBr addition (Fig. 5C), conditions under which the yield of benzene to $PhN(SiMe_3)_2$ was 68 ± 4% per iron. Toluene gave a mixture of (*m*-tolyl)$N(SiMe_3)_2$ and (*p*-tolyl)$N(SiMe_3)_2$ in a 3:1 ratio with a total yield of 61 ± 7% per iron. The overall yield is similar to that for benzene, and the ratio of isomers is comparable to that observed in the crystal of LFe(H)(Tol)Na(15c5) (Fig. S54). When *o*-xylene was used, a 12 ± 2% yield of *N,N*-bis(trimethylsilyl-3,4-xylidine) was observed. These silylated aniline products could be hydrolyzed to the deprotected anilines with weak aqueous acid when desired. Arenes with easily reducible functionalities such as aryl halides, aryl ethers, and polycyclic aromatics did not give aminated products. Formation of the silylated aniline and $N(SiMe_3)_3$ also occurred with other Me_3SiX reagents as well (X = Cl, I, and OTf), though the reaction gave the highest yields with Me_3SiBr.

The strategy outlined here differs fundamentally from previously described strategies for formation of C–N bonds from N_2. Typically, carbon electrophiles have been used to create C–N bonds, either from N_2[13,42–46] or nitrides that result from cleavage of N_2[15–17,47]. In the new reaction, silylation plays a key role by making the coordinated N_2 sufficiently reactive to accept the migrating aryl group from the metal center. The silylated amines that are formed can be used in further synthetic steps or can be deprotected to the parent anilines using mild aqueous acid. In this method, the C–N bond comes from the migration of a

hydrocarbyl from a metal to an N_2-derived group, a strategy that has been used in few stoichiometric C–N bond formation reactions[18,48]. The ability of these iron complexes to generate a hydrocarbyl group on the iron through C–H activation and then transfer it to an activated N_2 provides a new tactic for coupling hydrocarbons to N atoms from atmospheric N_2, combining the powers of these bond-cleaving reactions.

Supplementary Material

Refer to Web version on PubMed Central for supplementary material.

Acknowledgments.

This research was supported by the U.S. Department of Energy, Office of Science, Office of Basic Energy Sciences, Catalysis Program, under Award DE-SC0020315 (final phases of the work), and by the National Institutes of Health under Award R01 GM-065313 (initial phases of the work). Additional fellowship support came from the National Institutes of Health (F31 GM-116463 to S.F.M.), the Netherlands Organization for Scientific Research (Rubicon Postdoctoral Fellowship 680-50-1517 to D.L.J.B.), and the EPSRC Centre for Doctoral Training in Critical Resource Catalysis (internship for C.J.V.H.). This work was supported in part by the facilities and staff of the Yale University Faculty of Arts and Sciences High Performance Computing Center, and by the National Science Foundation under Award CNS-08-21132 that partially funded acquisition of the HPC facilities. We thank Nilay Hazari, James Mayer, Jonathan Ellman, Kazimer Skubi, and the referees for critical feedback on the manuscript.

References

1. Kim S, Loose F & Chirik PJ Beyond Ammonia: Nitrogen-Element Bond Forming Reactions with Coordinated Dinitrogen, Chem. Rev 120, in press (2020).
2. McWilliams SF et al., Effects of N_2 binding mode on iron-based functionalization of dinitrogen to form an iron(III) hydrazido complex. J. Am. Chem. Soc 140, 8586–8598 (2018). [PubMed: 29957940]
3. Schlögl R Ammonia Synthesis, in Handbook of Heterogeneous Catalysis, Wiley, Weinheim, 2008, vol. 5, pp. 2501–2575.
4. Burgess BK & Lowe DJ Mechanism of Molybdenum Nitrogenase. Chem. Rev 96, 2983–3012 (1996). [PubMed: 11848849]
5. Hoffman BM, Lukoyanov D, Yang ZY, Dean DR & Seefeldt LC Mechanism of nitrogen fixation by nitrogenase: the next stage. Chem. Rev 114, 4041–4062 (2014). [PubMed: 24467365]
6. Schrock RR Catalytic reduction of dinitrogen to ammonia at a single molybdenum center. Acc. Chem. Res 38, 955–962 (2005). [PubMed: 16359167]
7. Chalkley MJ, Del Castillo TJ, Matson BD, Roddy JP & Peters JC Catalytic N_2-to-NH_3 Conversion by Fe at Lower Driving Force: A Proposed Role for Metallocene-Mediated PCET. ACS Cent. Sci 3, 217–223 (2017). [PubMed: 28386599]
8. Nishibayashi Y Development of catalytic nitrogen fixation using transition metal-dinitrogen complexes under mild reaction conditions. Dalton Trans 47, 11290–11297 (2018). [PubMed: 30087974]
9. Chen JG et al., Beyond fossil fuel–driven nitrogen transformations. Science 360, eaar6611 (2018). [PubMed: 29798857]
10. Andino JG, Mazumder S, Pal K & Caulton KG New Approaches to Functionalizing Metal-Coordinated N_2. Angew. Chem. Int. Ed 52, 4726–4732 (2013).
11. Hidai M & Mizobe Y Recent Advances in the Chemistry of Dinitrogen Complexes. Chem. Rev 95, 1115–1133 (1995).
12. MacKay BA & Fryzuk MD Dinitrogen Coordination Chemistry: On the Biomimetic Borderlands. Chem. Rev 104, 385–401 (2004). [PubMed: 14871129]
13. Mori M, Activation of nitrogen for organic synthesis. J. Organomet. Chem 689, 4210–4227 (2004).

14. Keane AJ, Farrell WS, Yonke BL, Zavalij PY & Sita LR Metal-Mediated Production of Isocyanates, R_3ENCO from Dinitrogen, Carbon Dioxide, and R_3ECl. Angew. Chem. Int. Ed 54, 10220–10224 (2015).
15. Figueroa JS, Piro NA, Clough CR & Cummins CC A nitridoniobium(V) reagent that effects acid chloride to organic nitrile conversion: synthesis via heterodinuclear (Nb/Mo) dinitrogen cleavage, mechanistic insights, and recycling. J. Am. Chem. Soc 128, 940–950 (2006). [PubMed: 16417385]
16. Curley JJ, Cozzolino AF & Cummins CC Nitrogen fixation to cyanide at a molybdenum center. Dalton Trans 40, 2429–2432 (2011). [PubMed: 21293816]
17. Klopsch I, Kinauer M, Finger M, Würtele C & Schneider S Conversion of dinitrogen into acetonitrile under ambient conditions. Angew. Chem. Int. Ed 55, 4786–4789 (2016).
18. Kakiuchi F & Chatani N Catalytic Methods for C-H Bond Functionalization: Application in Organic Synthesis. Adv. Synth. Catal 345, 1077–1101 (2003).
19. Davies HML, Du Bois J & Yu J-Q C–H Functionalization in organic synthesis. Chem. Soc. Rev 40, 1855–1856 (2011). [PubMed: 21390392]
20. Smith JM et al. Studies of low-coordinate iron dinitrogen complexes. J. Am. Chem. Soc 128, 756–769 (2006). [PubMed: 16417365]
21. Holland PL Electronic Structure and Reactivity of Three-Coordinate Iron Complexes. Acc. Chem. Res 41, 905–914 (2008). [PubMed: 18646779]
22. Kalman SE et al. Facile and Regioselective C–H Bond Activation of Aromatic Substrates by an Fe(II) Complex Involving a Spin-Forbidden Pathway. Organometallics 32, 1797–1806 (2013).
23. Hickey AK, Lutz SA, Chen C-H & Smith JM Two-state reactivity in C–H activation by a four-coordinate iron(0) complex. Chem. Commun 53, 1245–1248 (2017).
24. Yu Y, Brennessel WW & Holland PL Borane B–C bond cleavage by a low-coordinate iron hydride complex and N–N bond cleavage by the hydridoborate product. Organometallics 26, 3217–3226 (2007). [PubMed: 18725998]
25. Sellmann D & Weiss W First reaction of dinitrogen ligands with bases: reduction of coordinated dinitrogen by nucleophilic attack. Angew. Chem 89, 918–919 (1977).
26. Sellmann D & Weiss W Consecutive nucleophilic and electrophilic attack on nitrogen ligands: synthesis of azomethane from molecular nitrogen. Angew. Chem 90, 295–296 (1978).
27. Deegan MM & Peters JC Electrophile-promoted Fe-to-N_2 hydride migration in highly reduced Fe(N_2)(H) complexes. Chem. Sci 9, 6264–6270 (2018). [PubMed: 30123481]
28. Jacobs BP, Wolczanski PT, Jiang Q, Cundari TR & MacMillan SN Rare Examples of Fe(IV) Alkyl-Imide Migratory Insertions: Impact of Fe—C Covalency in (Me_2IPr)Fe(═NAd)R_2. J. Am. Chem. Soc 139, 12145–12148 (2017). [PubMed: 28796945]
29. Nishibayashi Y Recent Progress in Transition-Metal-Catalyzed Reduction of Molecular Dinitrogen under Ambient Reaction Conditions. Inorg. Chem 54, 9234–9247 (2015). [PubMed: 26131967]
30. Siedschlag RB et al., Catalytic silylation of dinitrogen with a dicobalt complex. J. Am. Chem. Soc 137, 4638–4641 (2015). [PubMed: 25799204]
31. Piascik AD, Li R, Wilkinson HJ, Green JC & Ashley AE Fe-Catalyzed Conversion of N_2 to $N(SiMe_3)_3$ via an Fe-Hydrazido Resting State. J. Am. Chem. Soc 140, 10691–10694 (2018). [PubMed: 30114921]
32. Tanabe Y & Nishibayashi Y Recent advances in catalytic silylation of dinitrogen using transition metal complexes, Coord. Chem. Rev 389, 73–93 (2019).
33. Lee Y, Mankad NP & Peters JC Triggering N_2 uptake via redox-induced expulsion of coordinated NH_3 and N_2 silylation at trigonal bipyramidal iron. Nat. Chem 2, 558–565 (2010). [PubMed: 20571574]
34. Tanaka H et al., Molybdenum-catalyzed transformation of molecular dinitrogen into silylamine: experimental and DFT study on the remarkable role of ferrocenyldiphosphine ligands. J. Am. Chem. Soc 133, 3498–3506 (2011). [PubMed: 21341772]
35. Yuki M et al., Iron-catalysed transformation of molecular dinitrogen into silylamine under ambient conditions. Nat. Commun 3, 1254 (2012). [PubMed: 23212383]
36. Liao Q, Saffon-Merceron N & Mézailles N N_2 reduction into silylamine at tridentate phosphine/Mo center: catalysis and mechanistic study. ACS Catal 5, 6902–6906 (2015).

37. Liao Q, Cavaillé A, Saffon-Merceron N & Mézailles N Direct synthesis of silylamine from N_2 and a silane mediated by a tridentate phosphine molybdenum fragment. Angew. Chem. Int. Ed 55, 11212–11216 (2016).
38. Prokopchuk DE et al., Catalytic N_2 reduction to silylamines and thermodynamics of N_2 binding at square planar Fe. J. Am. Chem. Soc 139, 9291–9301 (2017). [PubMed: 28613896]
39. Suzuki T et al., Efficient catalytic conversion of dinitrogen to $N(SiMe_3)_3$ using a homogeneous mononuclear cobalt complex. ACS Catal 3011–3015 (2018).
40. Ferreira RB et al., Catalytic Silylation of Dinitrogen by a Family of Triiron Complexes. ACS Catal 8, 7208–7212 (2018). [PubMed: 30574427]
41. Gómez-Gallego M & Sierra MA Kinetic Isotope Effects in the Study of Organometallic Reaction Mechanisms. Chem. Rev 111, 4857–4963 (2011). [PubMed: 21545118]
42. Hidai M & Mizobe Y Recent Advances in the Chemistry of Dinitrogen Complexes. Chem. Rev 95, 1115–1133 (1995).
43. Betley TA & Peters JC Dinitrogen Chemistry from Trigonally Coordinated Iron and Cobalt Platforms. J. Am. Chem. Soc 125, 10782–10783 (2003). [PubMed: 12952446]
44. Bernskoetter WH, Olmos AV, Pool JA, Lobkovsky E & Chirik PJ N-C Bond Formation Promoted by a Hafnocene Dinitrogen Complex: Comparison of Zirconium and Hafnium Congeners. J. Am. Chem. Soc 128, 10696–10697 (2006). [PubMed: 16910661]
45. Knobloch DJ, Lobkovsky E & Chirik PJ Dinitrogen cleavage and functionalization by carbon monoxide promoted by a hafnium complex. Nat. Chem 2, 30–35 (2009). [PubMed: 21124377]
46. Moret M-E & Peters JC N_2 functionalization at iron metallaboratranes. J. Am. Chem. Soc 133, 18118–18121 (2011). [PubMed: 22008018]
47. MacLeod KC et al., Alkali-Controlled C–H Cleavage or N–C Bond Formation by N_2-Derived Iron Nitrides and Imides. J. Am. Chem. Soc 138, 11185–11191 (2016). [PubMed: 27571271]
48. Morello L, Love JB, Patrick BO & Fryzuk MD Carbon-Nitrogen Bond Formation via the Reaction of Terminal Alkynes with a Dinuclear Side-on Dinitrogen Complex. J. Am. Chem. Soc 126, 9480–9481 (2004). [PubMed: 15291518]

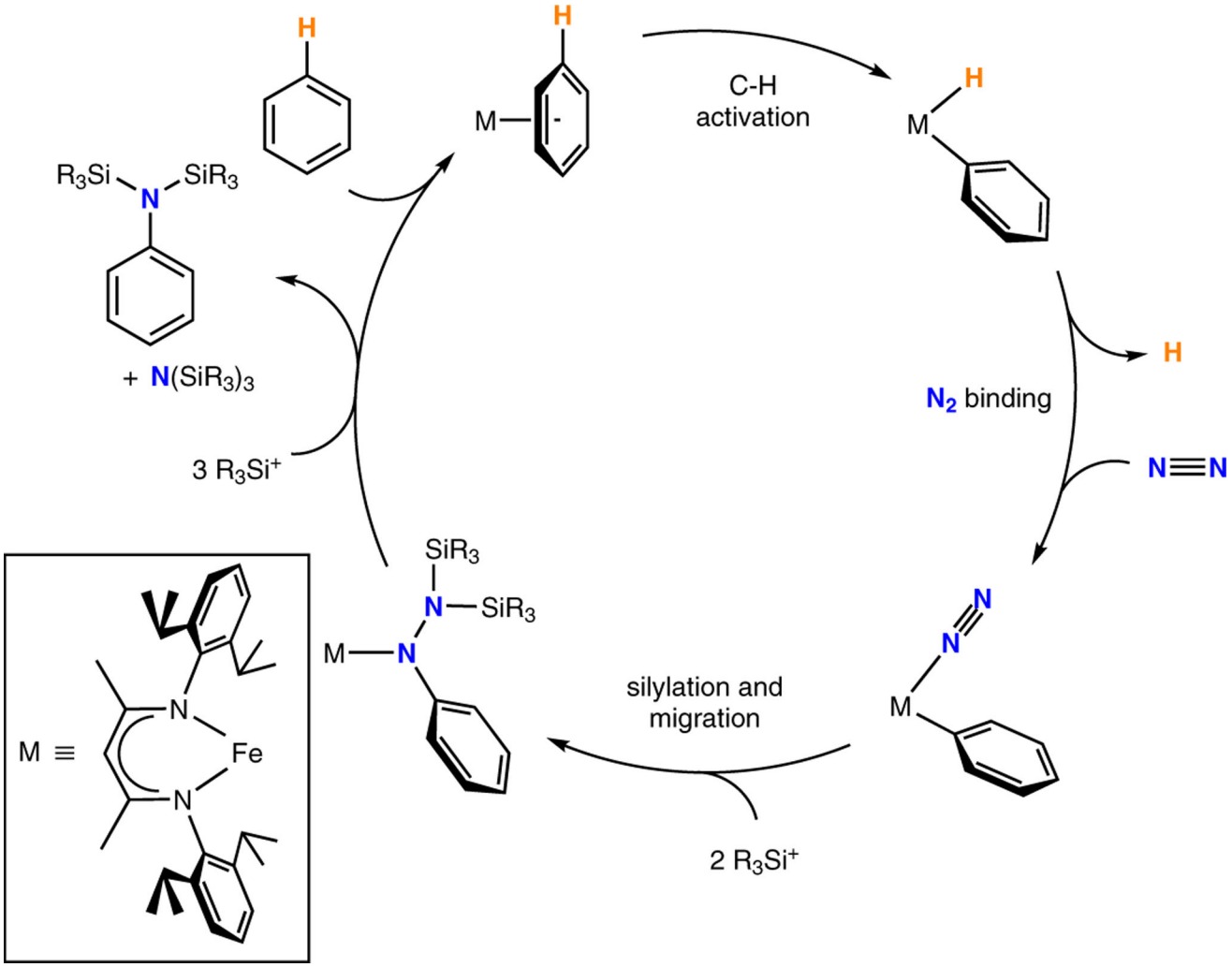

Fig. 1. Strategy for converting benzene and N_2 into silylated aniline without the use of carbon electrophiles.

Reduction steps are not shown here for simplicity, but are elaborated in Fig. 4 below. Inset: the iron β-diketiminate fragment used in this implementation of the strategy.

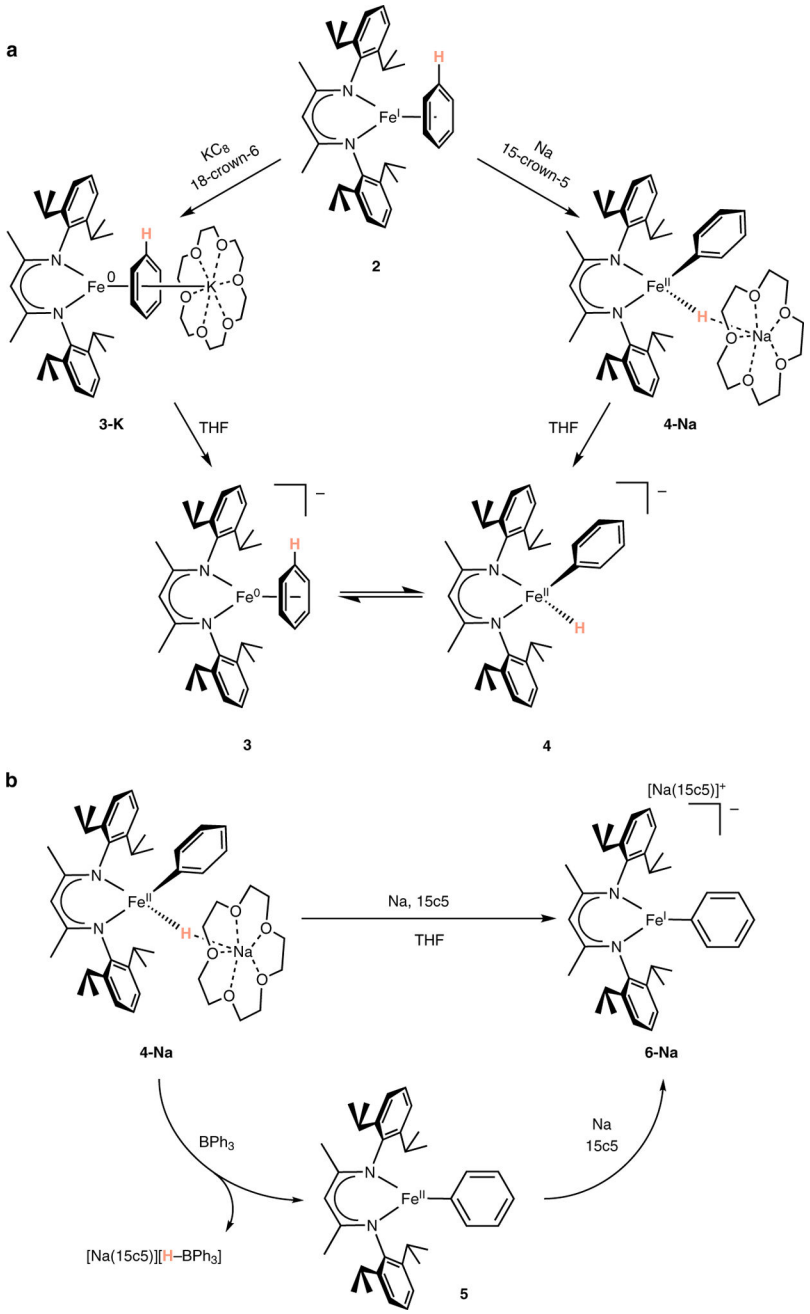

Fig. 2. Activation of benzene.

(a) Reduction of **2** with KC_8/18c6 formed **3-K** (left) while reduction with Na/15c5 formed **4-Na** (right). In THF solvent the cations dissociate, and isomeric anions **3** and **4** are in equilibrium. (b) Conversion of **4-Na** to **6-Na** occurred spontaneously in 18% yield (top pathway), but gave a higher yield of 75% with the hydride acceptor BPh_3 (bottom pathway), suggesting that hydride loss is likely to be the main reaction pathway.

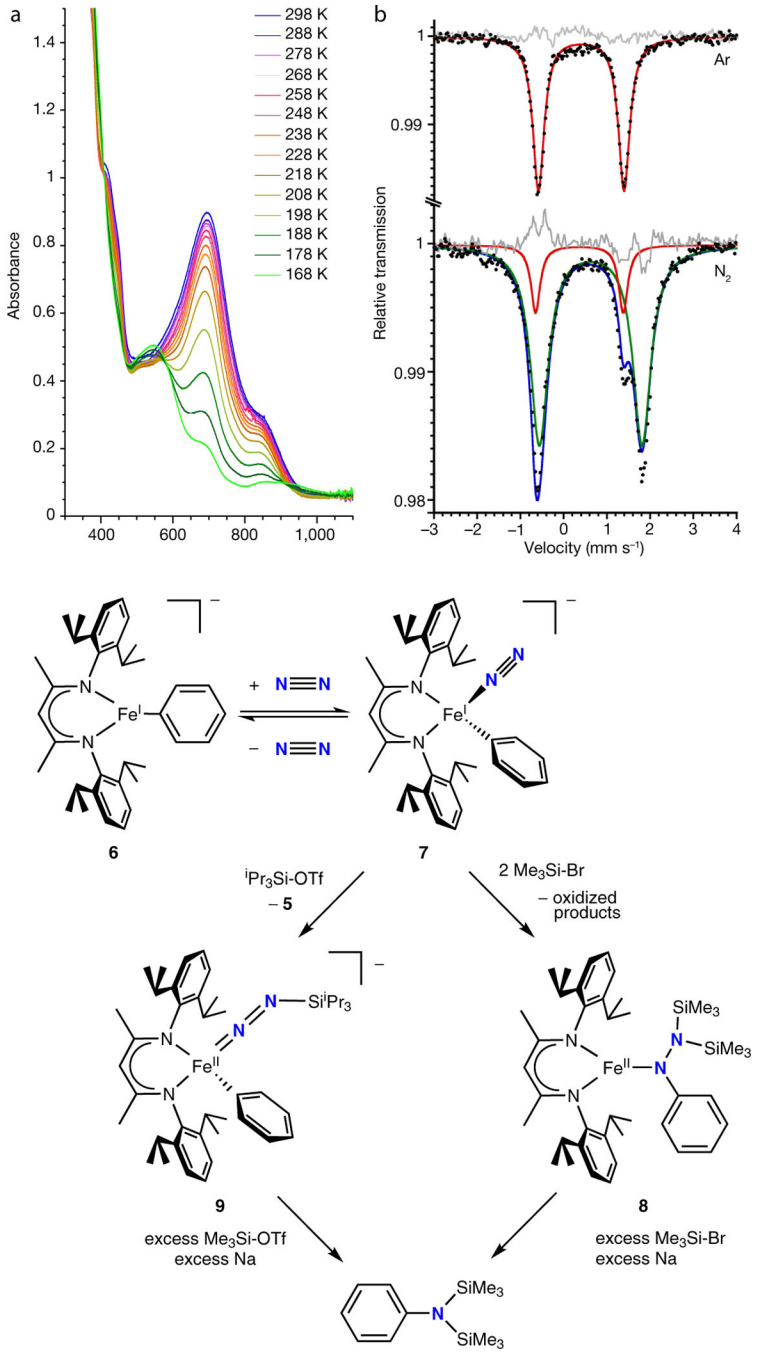

Fig. 3. Binding and functionalization of N_2.

(a) Electronic absorption spectra of **6-Na** in THF solution at various temperatures under 1 atm N_2, demonstrating the formation of **7-Na** at lower temperature. The data for **6-K** are similar (Fig. S37). (b) ^{57}Fe Mössbauer spectra at 80 K, from samples of **6-K** in THF solution frozen under 1 atm Ar (top) or 1 atm N_2 (bottom), demonstrating the formation of a new doublet attributed to the N_2 complex **7-K** (green subspectrum) in addition to some remaining **6-K** (red subspectrum). (c) Illustration of the equilibrium of **6** and N_2 to form **7**. In a key transformation, silylation of the bound N_2 in **7** induces migration of the phenyl

group to the N_2 fragment, giving **8**. When a bulkier silyl group is used, it is possible to isolate the singly silylated species **9**, which can subsequently form C–N bonds. Each of the iron species has been characterized through X-ray crystallography (Fig. 4 and S50–S55).

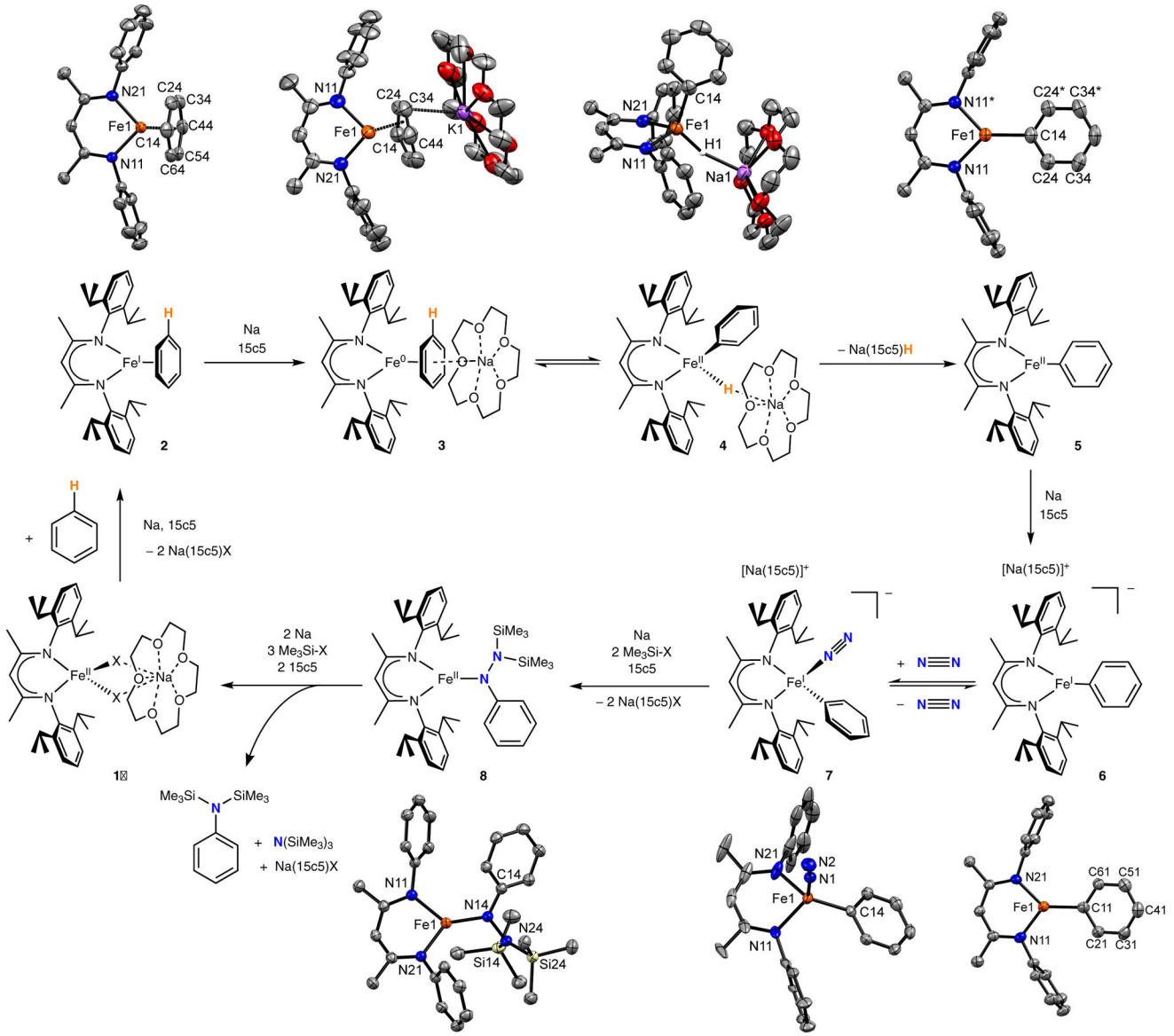

Fig. 4. Proposed cyclic reaction mechanism for the conversion of N_2 and benzene to aniline mediated by iron β-diketiminate complexes.

Thermal ellipsoid plots of the isolated intermediates are shown on the outside of the cycle (for ionic compounds, only the anion is shown). Hydrogen atoms and isopropyl groups are omitted from the thermal ellipsoid plots for clarity.

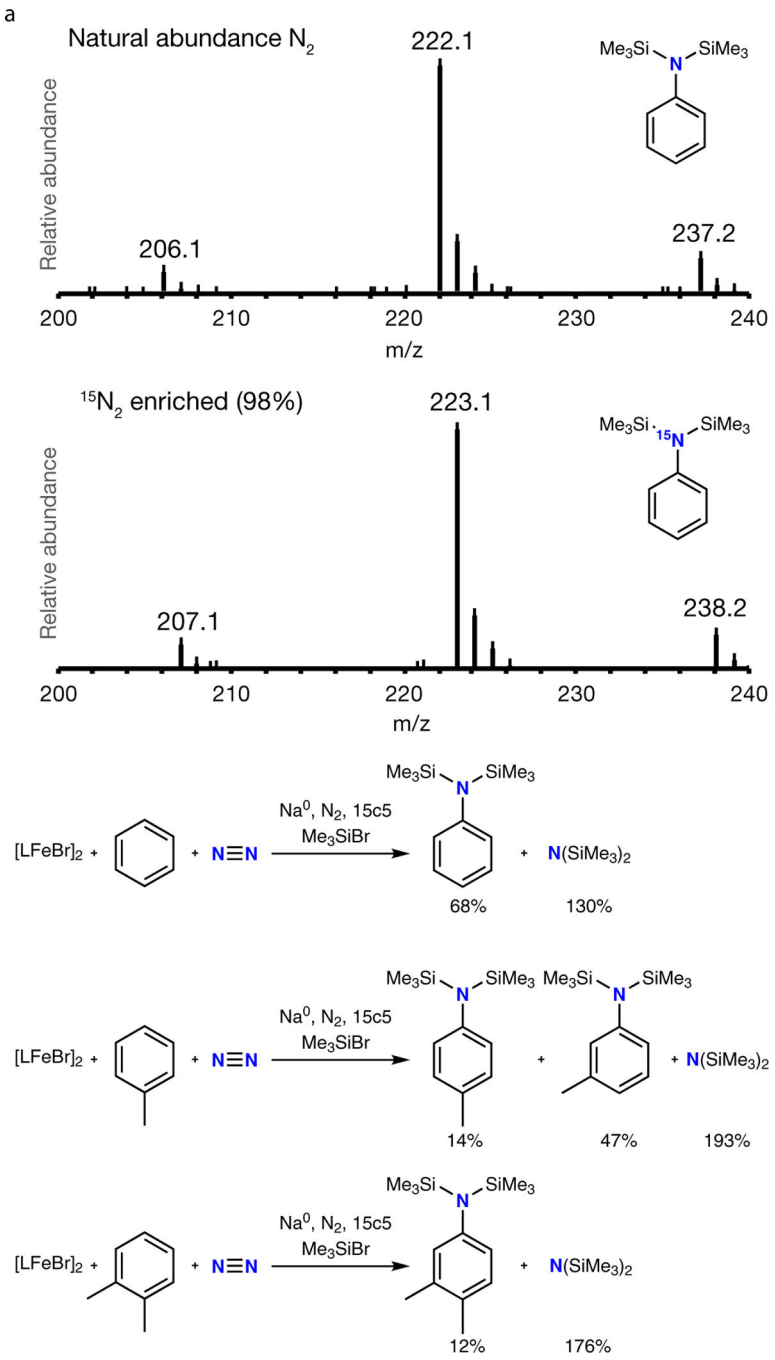

Fig. 5. Aniline products from amination of arenes with N_2.

(a) Mass spectra of $PhN(SiMe_3)_2$ products from reaction under 1 atm of natural abundance N_2 (top) and from reaction under 1 atm of $^{15}N_2$ (bottom), showing that the nitrogen atom in the product derives from N_2. (b) Yields (relative to Fe) of N-containing products during N_2-based amination of different arenes, using 5 cycles of Me_3SiBr addition (2 equivalents per cycle).